



Biocatalytic efficacy of chitosan microsphere-embedded lipase on long-chain fatty acid ester pollutants in water

Yan Zhu^{1,*}

¹ School of Resources and Environmental Engineering, Yangzhou Polytechnic College, Yangzhou, Jiangsu, 225008, China

SUMMARY: *Immobilized lipase, as a hot research field of enzyme engineering, can effectively overcome the shortcomings of natural enzymes such as unstable, easy to inactivate and difficult to reuse. In this paper, chitosan microspheres were prepared from chitosan and modified with succinic anhydride to obtain a series of N-succinyl chitosan with different degrees of substitution. The N-succinyl chitosan microspheres were used as carriers, and the microspheres were fully solubilized and immobilized with lipase by the embedding method. The effects of pH and cross-linking temperature on the immobilized enzyme activity were explored to determine the optimal experimental environmental parameters. Hydrolysis experiments were designed to characterize the biocatalytic efficacy of lipase for hydrolysis of long-chain fatty acid ester pollutants using olive oil. The optimal reaction pH and the optimal cross-linking temperature for the immobilized lipase were measured to be 7.5 pH and 48 °C, respectively. After catalytic hydrolysis for 40 min, the degradation efficiency of the immobilized lipase for long-chain fatty acid ester pollutants reached about 1.6 times that of the free lipase, with an efficiency as high as 70.12%.*

KEYWORDS: *chitosan microspheres; embedded lipase; long-chain fatty acid esters; biocatalysis; N-succinyl chitosan; pollutants*

1 Introduction

Currently, chemical, pharmaceutical, and food industries, sewage treatment plant discharges, and agricultural pollution result in the discharge of thousands of chemical pollutants into rivers and streams, such as polycyclic aromatic hydrocarbon pollutants, organic acids, fatty acids, ketones, esters, and other compounds [1-4]. In addition, although all urban domestic wastewater is treated in sewage treatment plants before discharge, there are still many organic pollutants after treatment in conventional sewage plants, while phthalates, phenols, and other organic pollutants in garbage leachate can have an impact on the environment [5-7]. Among them, long-chain fatty acid (LCFA) ester pollutants as organic pollutants are more stable in chemical structure and difficult to be completely degraded by traditional wastewater treatment methods [8]. After these organic chemical pollutants enter the water environment, if their content exceeds the self-purification capacity and background value of the water body, it will make the water quality damaged, destroy the biological community in the water, cause eutrophication, deteriorate the quality of the water body's substrate, affect the original use and nature of the water body, and have a potentially adverse effect on human health [9-11].

Many pollutants in the chemical treatment will also generate more difficult to degrade toxic

*18852896128@163.com

<https://doi.org/10.65102/is2026042>

and harmful substances, causing secondary pollution to the environment, but the physical method only treats the symptoms but not the root cause. Biocatalytic technology, however, is widely recognized as an effective, economical and highly ecological high-tech environmental technology in the field of large-scale pollution treatment because it overcomes the shortcomings of chemical and physical methods [12-14]. Among them, the lipase enzyme is immobilized on a suitable carrier to form immobilized lipase, which is a special ester-bond hydrolase that can carry out catalytic lipolysis, ester exchange, ester synthesis and other reactions, which provides a reference for the efficient degradation of a variety of esters.

Maghraby et al [15] reported that the immobilization techniques for enzymes are covalent binding, encapsulation, embedding, and adsorption, and these types of enzymes have greater resistance to environmental changes, as well as enzyme reusability and recyclability. Some of the enzyme immobilization techniques are effective in degrading various pollutants. Liu and Dave [16] outlined the performance of enzyme immobilization techniques, whose activity and stability are affected by the carrier and immobilization method, and indicated that immobilized lipases are capable of catalyzing the hydrolysis and alcoholysis of ω -3 fatty acids in fish oil. Alzahrani et al [17] conducted wastewater treatment tests and on day 9, the immobilized enzyme was able to completely remove lipids, which was twice as effective as the unimmobilized enzyme, and significantly reduced COD and residual lipid levels. Zong et al [18] introduced a novel esterase (Est882) and revealed that the immobilized esterase was able to efficiently hydrolyze pyrethroid residues and industrial ester pollutants, which contributes to bioremediation. Işık et al [19] proposed a novel bioremediation method for the removal of wastewater containing high oleic acid content by immobilizing *Fusobacterium haemolyticum* lipase on eggshell membranes to improve enzyme activity and stability.

Chitosan microspheres are biocompatible, non-toxic, and easily degradable, and for immobilizing lipase on chitosan microspheres, scholars have proposed a variety of preparation schemes. N-succinyl chitosan bead-immobilized bovine pancreatic lipase prepared by Cui et al [20] was effective in enriching polyunsaturated fatty acids in fish oils with an initial activity and an activity of 1480 U/g and 1134 U/g (76.6% of the original) after five recoveries, respectively. Tu et al [21] used immobilization by adsorption between lipase and chitosan/clay in olive oil hydrolysis, which resulted in higher activity and stability of the fatty acid hydrolysis process, and higher catalytic performance could be obtained for chitosan+clay-embedded fatty acids. Melo et al [22] immobilized lipase on a hybrid microcarrier consisting of chitosan and sodium phosphate, which showed reproducible applicability, catalytic recovery, and dynamic temperature stability, and improved catalytic activity increment in transesterification reactions. Weng et al [23] prepared a lipase/chitosan nanoparticle-based catalyst for water-in-oil Pickering emulsions, which reached 72.80% hydrolysis rate for olive oil hydrolysis for 12 min and as high as 99.62% for 120 min, while chitosan nanoparticle-immobilized lipase showed excellent reusability and activity. Pereira et al [24] combined chitosan and alginate as carriers to achieve immobilization of extracellular lipase from the yeast *Populus flavus* under ionic cross-linking method, with a pH value of 7.5-8 and an optimum reaction temperature of 35°C-40°C, and its microencapsulation provided higher thermal stability. Costa-Silva et al [25] immobilized lipase on chitosan beads by fluidized bed technique in combination with benzoyl peroxide activation, which retained 75.2% of the original activity even after 10 repetitions, and catalyzed the esterification reaction to produce butyl butyrate. Akil et al [26] catalyzed and immobilized anthropomorphic thin-walled yeast lipase in chitosan-alginate microspheres under solvent-free conditions using acidolysis reaction made as a biocatalyst with good performance and potential. Liu et al [27] employed the cohesive interaction between lipase and chitosan to produce chitosan microsphere-lipase, which is highly porous and thermally stable, and increased the

maximum rate of enzymatic reaction by 2.4 times.

The chitosan microsphere-lipase can obtain higher activity, stability, reusability and antioxidant properties, which is in line with the green and sustainable concept of biocatalytic technology and opens up a new pathway for the degradation of LCFA ester pollutants. Wei et al [28] applied an ionic cross-linking method to modify magnetic chitosan nanoparticles and combined two lipases and tween to design a one-pot co-immobilization method capable of catalyzing waste animal fats and oils into biodiesel. Ribeiro et al [29] developed microstructured chitosan nanocapsules with immobilized lipase, which presented optimal reusability and excellent cost-effectiveness during the hydrolysis of nitrobenzoic acid palmitate at 37°C and pH=8. However, Charuwat et al [30] implemented a thermal degradation test of LCFA for 30 min-8 h. The saturated LCFA degraded to C2 to C14 after 8 h. The saturated LCFA with biocatalysts remained stable, while the unsaturated LCFA was almost completely degraded. In addition, chitosan microspheres are fragile and the enzyme activity is easily inhibited by the mixture of pollutants in complex water bodies. Therefore, further development of more efficient and stable chitosan microsphere-embedded lipase technology is needed to achieve excellent catalytic efficacy for LCFA ester pollutants for waterbody remediation.

In this paper, three experiments were set up to fully explore the advantages of chitosan microsphere-embedded lipase in the catalytic degradation of long-chain fatty acid ester pollutants in water. Experiment 1 was the preparation of N-succinyl chitosan microspheres, based on the determination of chitosan deacetylation degree, chitosan gel microspheres with different mass fractions were prepared. The N-succinyl chitosan microspheres were obtained by adding succinic anhydride/anhydrous ethanol solution and stirring the square sound to obtain N-succinyl chitosan with different degrees of substitution. Experiment 2 investigated the curing effect of lipase on the prepared N-succinyl chitosan. The curing method was the embedding method, in which the lipase phosphate solution was added to the dissolved chitosan microsphere solution, and the lipase was successfully cured by shaking bed shaking and precipitation operations. Experiment 3 verified the biocatalytic efficacy of immobilized lipase. Olive oil was used as the hydrolysis target, and the immobilized enzyme was combined with the Mie equation to characterize the degradation efficiency of long-chain fatty acid ester pollutants in water.

2 Preparation and analysis of N-succinyl chitosan microspheres

N-succinyl chitosan has good degradability, biocompatibility, antibacterial and antimicrobial properties, low toxicity, film-forming properties and other characteristics. Chitosan is a rich source, cheap and contains a large number of active amino and hydroxyl groups, with significant affinity, metal ion chelating and other biochemical properties, making it an ideal carrier for enzyme immobilization.

2.1 Experimental Methods

2.1.1 Determination of Deacetylation of Chitosan

The free amino group of chitosan is weakly basic and can protonate quantitatively with acid to form a colloidal solution of chitosan. The protonation of chitosan is shown schematically in Figure 1. The excess acid in the colloidal solution can be back-titrated with a base, and the amount of free amino groups in chitosan can be deduced from the difference between the acid and base amounts.

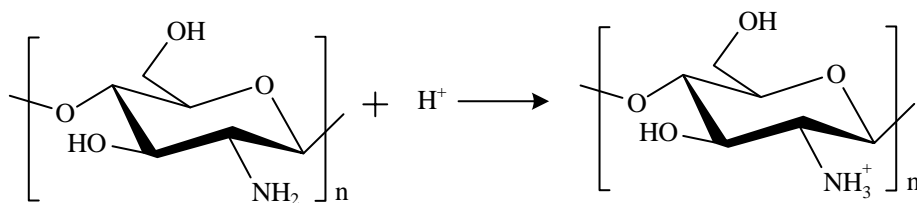


Figure 1: Protonation scheme of chitosan

Accurately weighing about 0.45 g of the sample in a 255 ml conical flask, add 0.2 mol / L of hydrochloric acid solution 25.6 mL, to be completely dissolved chitosan, with 0.15 mol / L of sodium hydroxide solution titration of chitosan solution in the excess of hydrochloric acid, methyl orange as an indicator. Another sample was taken in the oven at 106°C, baked to constant weight, and the moisture W was determined, and the determination was repeated three times to take the average value. Calculate the water content and deacetylation degree according to the following formula:

$$\%NH_2 = \frac{(C_1V_1 - C_2V_2 \times 0.016)}{G(100 - W)} \times 100\% \quad (1)$$

$$D.D.\% = \frac{\%NH_2}{9.94\%} \times 100\% \quad (2)$$

In the formula:

C_1 -concentration of hydrochloric acid standard solution (mol/L);

V_1 -volume of hydrochloric acid standard solution added (mL);

C_2 -concentration of sodium hydroxide standard solution (mol/L);

V_2 -volume of sodium hydroxide standard solution consumed during titration (mL);

G -weight of specimen (g);

W - moisture of specimen (%);

0.016-ammonium equivalent to 1mL of 1mol/L hydrochloric acid solution;

9.94%-Theoretical amine content.

2.1.2 Preparation of chitosan microspheres

Firstly, a certain amount of chitosan powder was weighed and dissolved in 2.5% glacial acetic acid, and the chitosan solutions with mass fractions of 1.5%, 2.5%, 3.5%, and 4.5% were prepared respectively, and magnetically stirred for 4.2 h at room temperature to make the chitosan fully soluble, and then stood overnight to remove the air bubbles. The configured chitosan solution was added drop by drop to an equal volume of 2~4 mol/L NaOH condensate through a syringe to form chitosan gel microspheres, which were condensed for 2.2 h at room temperature, and then rinsed repeatedly with deionized water to neutrality to obtain the size-uniform milky white chitosan microspheres.

2.1.3 Preparation of N-succinyl chitosan microspheres

N-succinylated chitosan is a derivative of N-acylated chitosan containing carboxyl groups, and a series of N-succinylated chitosans with different degrees of substitution can be prepared by controlling the reaction time. The synthetic route of N-succinylated chitosan microspheres is shown in Fig. 2.3.2g of chitosan microspheres were added to a 120 ml three-necked flask, and

then succinic anhydride/anhydrous ethanol solution was added (4.5g of succinic anhydride dissolved in 75 ml of anhydrous ethanol), magnetic stirring, and the reaction was carried out at 65 °C for 13.4 h. After the reaction, the solid phase was soaked in ethanol for 8 h. After filtration, the solid phase was washed repeatedly with ethanol and dried in vacuum at 65 °C for 36 h, which led to N-succinimidyl chitosan microspheres with different degrees of substitution.

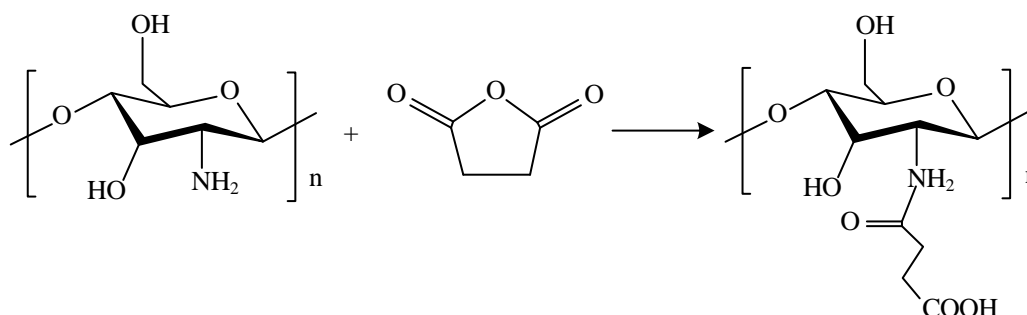


Figure 2: Synthesis of N-succinyl-chitosan

2.2 Characterization methods

2.2.1 Fourier infrared spectral analysis

The chitosan microspheres before and after graft modification were ground into fine powder form and then mixed with KBr at a ratio of about 1:160, and then pressed to obtain transparent thin slices, and the FTIR spectra were plotted on an infrared spectral analyzer with a scanning wavelength in the range of 5000-300 cm^{-1} and a scanning speed of 2.5 cm^{-1} . Accordingly, the preparation process of chitosan resin and the changes of each part of the groups before and after graft modification were analyzed.

2.2.2 Nuclear magnetic resonance characterization

The compositional structure of N-succinyl chitosan was analyzed by nuclear magnetic resonance spectroscopy (NMR/500 MHz). Heavy water was used as solvent and tetramethylsilane as internal standard.

2.2.3 X-ray diffraction characterization

The X-ray diffraction test was performed at a scanning speed of 8°/min and a scanning range of 4°-65°.

2.3 Results and Discussion

2.3.1 Fourier infrared spectral analysis

The prepared N-succinyl chitosan and chitosan microspheres were characterized by Fourier transform infrared spectroscopy (FTIR). The FTIR characterization results are shown in Figure 3. The stretching vibration peak of $-\text{NH}_2$ was 3800-4300 cm^{-1} , and no peak was observed in this wavelength range in the following figure. This is because the acetyl groups in the chitosan molecule are affected by intermolecular or intramolecular hydrogen bonds. The peak at 3820 cm^{-1} in the above figure indicates that an acylation reaction has occurred at the $-\text{NH}_2$ position in the chitosan molecule. Due to the stretching vibrations of $-\text{OH}$ and $-\text{NH}_2$ in the chitosan molecule, the lower graph shows vibrational peaks at 3400-3750 cm^{-1} . After succinylation reaction occurs, the peak in the above graph narrows in this wavelength range.

The absorption peaks of C=O (amide I) at 1438 cm^{-1} and N-H (amide II) at 787 cm^{-1} appear in the upper graph, which indicates the presence of -NH-CO- structure in N-succinylated chitosan. It can be seen that the reaction of chitosan with succinic anhydride resulted in the appearance of -NH-CO structure in the product.

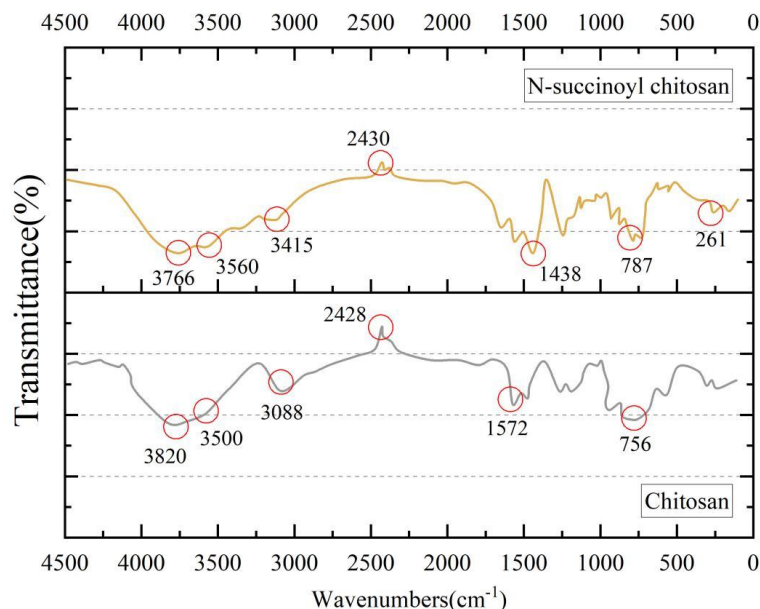


Figure 3: Fourier transform infrared spectroscopy analysis

2.3.2 Nuclear magnetic resonance characterization

Figure 4 shows the measured NMR spectra of N-succinyl chitosan hydrogen. The H in the acetyl group causes chitosan to peak in the chemical shift range of 1.80-1.95 ppm, but after succinylation, the peaks in this range are significantly weakened. N-succinyl chitosan did not show a significant peak at 1.80-1.95 ppm. N-succinyl chitosan showed distinct peaks near chemical shifts 2.25-2.5 ppm and 3.83 ppm due to the presence of -NHC₂H₄COOH. N-succinyl chitosan showed peaks at chemical shifts of 2.0-2.25 ppm, which were generated by H in -CH₂CH₂-. The appearance of these peaks proves the occurrence of N-acylation reaction. This is in agreement with the results of FTIR analysis.

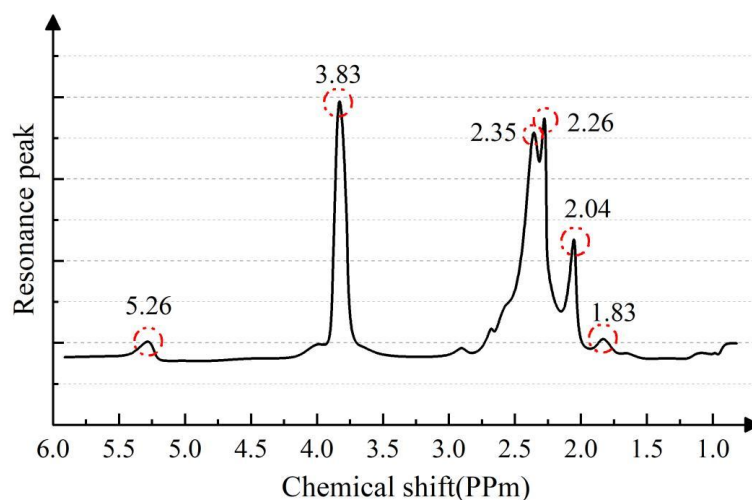


Figure 4: The nuclear magnetic resonance hydrogen spectrum of N-succinyl chitosan

2.3.3 X-ray diffraction characterization

Using X-ray diffraction test scans, the X-ray diffraction curves of chitosan and N-succinyl chitosan are shown in Figure 5. In Fig. 5, the characteristic diffraction peaks of chitosan appeared at $2\theta=11^\circ$ and $2\theta=25^\circ$ in the a curve, and there was no diffraction peak at $2\theta=11^\circ$ in the b curve, and the intensity of the diffraction peaks at $2\theta=25^\circ$ was smaller. This is because the transformation of $-\text{NH}_2$ to $-\text{NH}-\text{CO}-$ in chitosan results in the disruption of hydrogen bonding in the chitosan molecule, weakening of ordering, and reduction of crystallinity, which is also responsible for the enhancement of the water solubility of N-succinyl chitosan.

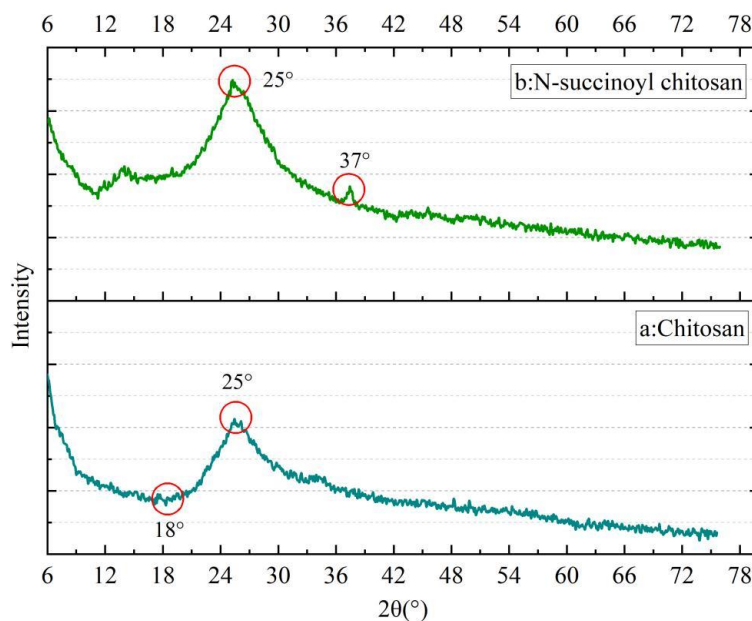


Figure 5: X-ray diffraction patterns of chitosan and N-succinyl-chitosan

3 Embedding curing and analysis of lipases

3.1 Experimental methodology

3.1.1 Embedding curing of lipases

Weighing 120 mg of microspheres, activated with 3.2% glutaraldehyde solution for 3 h. Wash it repeatedly with ultrapure water for 6 times, then add it into 110 mL conical flasks, and dissolve it fully with phosphate buffer solution of pH 7.0 for 36 h. Then, precipitate it completely with a strong magnet, discard the supernatant, and then wash it repeatedly with ultrapure water for 6 times. The solubilized magnetic chitosan microspheres were added into 0.25% lipase phosphate solution (prepared with pH8.2, 0.3 mol/L buffer), and the shaker was shaken at a constant temperature of 16 °C for a certain period of time, and the magnetic chitosan microspheres were precipitated with a strong magnet, separated, and washed with pH8.2, 0.15 mol/L buffer for 6 times, and then washed repeatedly with ultrapure water for 6 times, and the immobilized enzyme was finally obtained, and was stored in the 4.5°C refrigerator for storage.

3.1.2 Determination of immobilized enzyme activity

The immobilized lipase activity was determined using the polyvinyl alcohol emulsified olive oil method. One unit of lipase activity was defined as the amount of enzyme that catalyzes the production of 1.2 μmol of fatty acids per minute from the hydrolysis of olive oil by lipase at pH

8.0 and 36 °C. The amount of fatty acids produced in the reaction was calculated from the acid-base reaction balance equation.

The specific steps are as follows: accurately prepare an aqueous solution of polyvinyl alcohol (PVA) with a mass fraction of 2.1%, mix it with olive oil according to 6:1(v/v) and place it in an ice-water bath and cool it to 12°C, and then stir it strongly with a stirrer for 25min, which is the milky-white PVA olive oil emulsion (substrate). Take 2.5mL 0.2mol/L pH7.0 phosphate buffer and 2.5mL substrate in a conical flask, mix them thoroughly, heat the water bath to 36°C and constant for 15min, then add 0.52mL 2% lipase, timing at the same time, stirring gently, and holding the reaction for 45min, then add 5.8mL acetone-ethanol mixture (v:v=1:1) to terminate the reaction, then add 5.8mL 0.1mol/L NaOH standard solution, 3 drops of 1% phenolphthalein indicator, and titrate with standard hydrochloric acid with molar concentration of 0.1mol/L until the solution is colorless, which is the end point.

The assay method and procedure for the control sample were the same as above, except that 5.8mL of acetone-ethanol mixture was added before enzyme addition (v:v=1:1). The determination of immobilized enzyme was the same as above, except that 0.15g of immobilized enzyme was added.

3.1.3 Viability recovery of immobilized enzymes

The viability recovery of magnetically immobilized enzyme is the ratio of the total viability of the immobilized enzyme to the total viability of the coupled free enzyme added to the immobilization process, expressed as a percentage.

$$\text{Enzyme activity recovery} = \frac{\text{Immobilized enzyme activity}}{\text{Enzyme activity after adding coupling enzyme solution}} \times 100\% \quad (3)$$

The relative activity of a magnetically immobilized or free enzyme is defined as the ratio of the activity of the highest activity of 100 to the activity of the remaining immobilized or free enzymes in the same group of tests, usually expressed as a percentage.

3.1.4 Optimum reaction temperature

Enzyme reaction activity is very sensitive to temperature, which can affect the chemical reaction rate itself, the stability of the enzyme, the thermal denaturation of enzyme proteins, but also the conformation of the enzyme and the catalytic mechanism of the enzyme. The so-called optimal temperature is actually the result of the combined influence of these factors.

Take two 120mL conical flasks labeled with *A*, *B*, each add 3.5mL of substrate and 2.5mL of 0.25mol/LpH8.0 phosphate buffer, *A* flask add 120mg of immobilized lipase, *B* flask add 0.25mL of lipase solution with a mass fraction of 3%, and respectively, the reaction was carried out by oscillating at 36°C in a constant temperature water bath for 7.5min After that, the enzyme activity of free enzyme and magnetic immobilized enzyme was determined by polyvinyl alcohol emulsified olive oil method.

The enzyme activities of free enzyme and magnetically immobilized enzyme were sequentially determined at 35, 45, 50, 55, 60 and 65°C by this method. The relative activity of free enzyme and magnetically immobilized enzyme means that the highest enzyme activity in the same group of tests is taken as 100%, and the relative activity of other free enzymes and magnetically immobilized enzymes is calculated accordingly, and the relative activity graph is made. In order to ensure the reliability and reproducibility of the results, the temperature was

strictly controlled within the range of $\pm 0.1^{\circ}\text{C}$.

3.1.5 Optimum Reaction pH

Sensitivity to environmental acidity and alkalinity is one of the characteristics of the enzyme, each enzyme can only show the maximum speed of enzyme reaction under certain conditions, usually called the optimal temperature of enzyme reaction.

Take two 120mL conical flasks labeled with *A*, *B*, each add 3.5mL of substrate and 2.5mL of phosphate buffer with a pH of 6.5, *A* flask add 120mg of activated magnetic immobilized lipase, *B* flask add 0.25mL of lipase solution with a mass fraction of 3%, and the reaction is carried out at a constant temperature of 55°C in a water bath with oscillation for 7.5min, and then the reaction is performed using the polyvinyl alcohol emulsified olive oil method to determine the enzyme activity of free enzyme and magnetic immobilized enzyme.

The enzyme activities of free enzyme and magnetically immobilized enzyme were sequentially determined at pH 7.0, 7.5, 8.0, 8.5, 9.0 and 9.5 by this method. The relative activity of free enzyme and magnetically immobilized enzyme means that the highest activity of the enzyme in the same group of tests is taken as 100%, and the relative activity of other free enzymes and magnetically immobilized enzymes is calculated accordingly, and the relative activity curve is made.

3.2 Results and Discussion

3.2.1 Effect of different PH on immobilized enzyme activity

The activity of immobilized lipase at different pH is shown in Fig. 6, and the substrate concentration tends to decrease with the extension of the reaction time, and the lowest substrate concentration was observed when the reaction time was 65 min. It can also be seen that the transesterification specific activity of immobilized lipase was higher when the pH of the phosphate solution was 7.5 than when the pH of the phosphate solution was 8.5, so the pH of the phosphate solution was chosen to be 7.5.

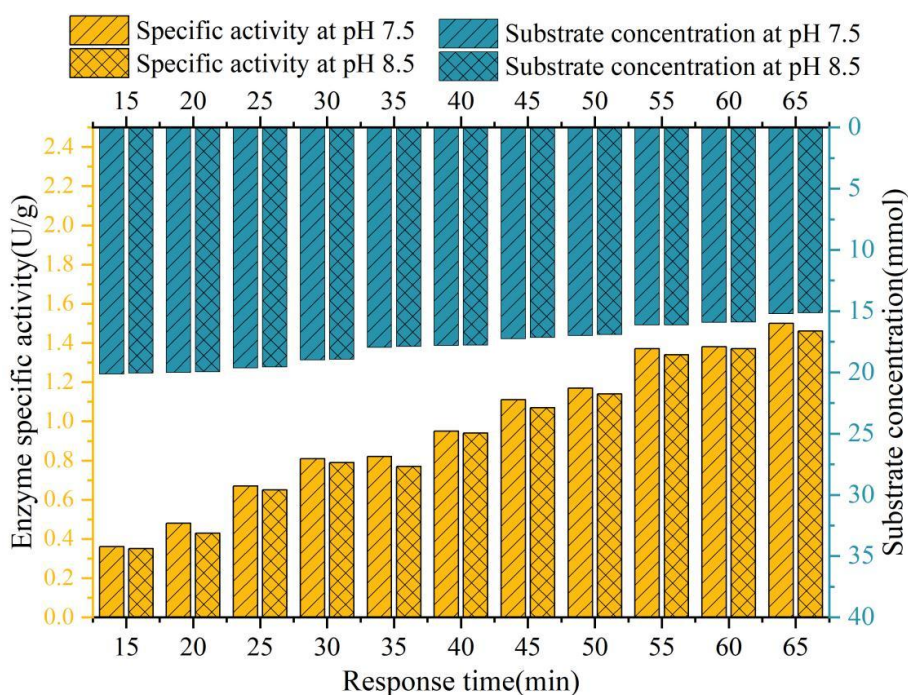


Figure 6: The activity of immobilized lipase at different pH values

The aggregation and precipitation of lipase is the driving force behind the immobilization of the enzyme on the washcloth. When a clear enzyme solution prepared in distilled water is mixed with a phosphoric acid solution, a cloudy, fuzzy, or “milky” suspension of phosphoric acid-enzyme aggregates forms instantly. This is due to the formation of an electrostatic complex between a highly branched, positively charged phosphate molecule and a negatively charged substance, such as a protein or nucleic acid.

3.2.2 Effect of crosslinking temperature on immobilized enzyme activity

Lipase aggregates were formed and temperature had an important effect. The effect of cross-linking temperature on chitosan-cured lipase is shown in Fig. 7. When the cross-linking temperature was lower than 48 °C, the transesterification specific activity of immobilized lipase increased gradually with the rise of temperature, and the transesterification specific activity of immobilized lipase was the highest at 48 °C, which reached 5.82 U/g of immobilized enzyme. However, when the temperature was higher than 48 °C, the transesterification specific activity of the prepared immobilized lipase decreased significantly. Therefore, the crosslinking temperature was selected as 48 °C.

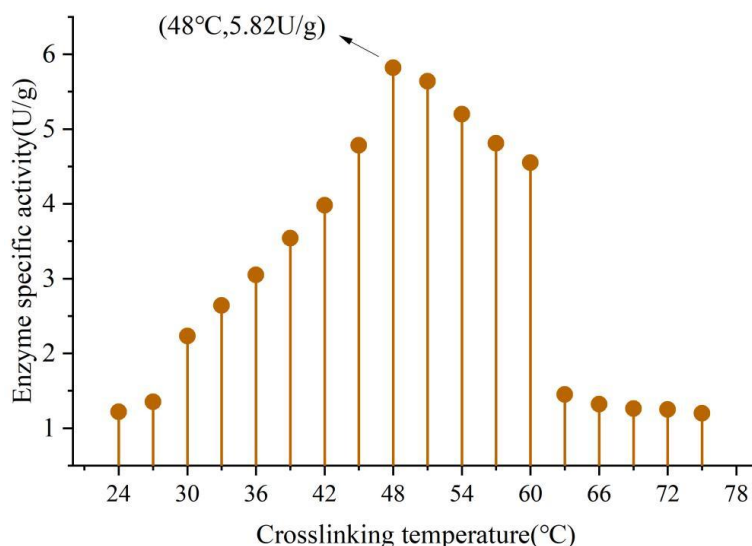


Figure 7: The influence of temperature to the activity of transesterification

4 Catalytic efficacy of chitosan-immobilized enzymes for acid-ester pollutants

4.1 Experimental methodology

According to Mie's equation (4), it can be seen that in order to determine the maximum reaction rate (V_{max}) and Mie's constant (K_m) of free and loaded lipase, the reaction rate of olive oil can be measured by measuring different concentrations (0.04-0.40 g/mL).

$$V = \frac{V_{max}[S]}{K_m + [S]} \quad (4)$$

$[S]$: concentration of olive oil (g/mL)

v : reaction rate of lipase-catalyzed hydrolysis of olive oil (mmol/min·L)

4.2 Results and Discussion

4.2.1 Immobilized Lipase-Catalyzed Long-Chain Fatty Acid Ester Contaminants

Lipase, as a green biocatalyst, can catalyze the degradation of a wide range of lipid compounds. In this chapter, long-chain fatty acid lipid pollutants, which are common in wastewater, were selected as catalytic substrates to evaluate the catalytic degradation performance of immobilized lipases. Figure 8 shows the degradation efficiencies of free and immobilized lipases for long-chain fatty acid lipid pollutants. It is noteworthy that the immobilized lipase degraded the long-chain fatty acid lipid pollutants as efficiently as 70.12% in 40 min, which is about 1.6 times higher than that of the free lipase. This is due to the interaction of degradation by-products with free lipase, which inhibits the catalytic reaction and leads to the impairment of free lipase activity. Moreover, after the immobilized lipase continued to react with the substrate for 3.5 h, the degradation efficiency of the long-chain fatty acid lipid pollutants was about 87.97%, which was about 17% higher than that of the first 40 min, which was due to the fact that a large amount of degradation products accumulated on the surface of the immobilized carrier, limiting the contact between the lipase and the substrate and affecting its degradation efficiency. The above results showed that the immobilized lipase with chitosan microspheres as the carrier as a biocatalyst could efficiently degrade long-chain fatty acid lipid pollutants.

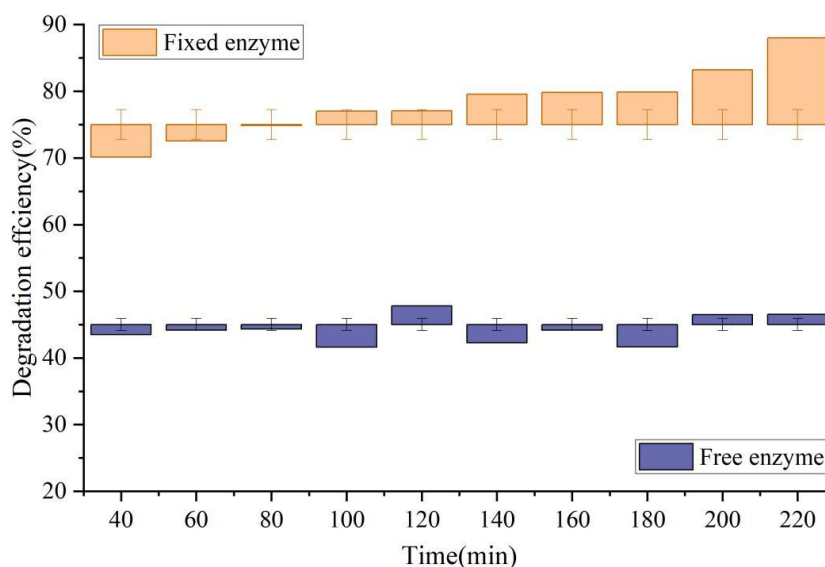


Figure 8: The catalytic efficiency of free lipase and immobilized lipase

4.2.2 Study of the degradation properties of the carrier

In the application of immobilized enzymes, the degradability of the carrier when the enzyme is inactivated is one of the main properties to judge the practical application of immobilized enzymes. In order to investigate the degradability of the immobilized carriers, unmodified lipase and immobilized carrier chitosan microspheres were mixed with 1.5 mol/L NaOH aqueous solution, respectively. Characterization was performed by scanning electron microscopy (SEC), and the results measured by SEC are shown in Figure 9. After 18 h of reaction in a strongly alkaline environment, the efflux time of the SEC elution peak of the pristine lipase moved from 12.40 min to 12.80 min only, and the correlation peak of the oligomeric small molecules obtained after degradation was observed at 20.8 min, indicating that the degradation of the pristine lipase was very slow. After the immobilized carrier was

treated with degradation, the efflux time of the polymer elution peak was significantly displaced and the molecular weight was significantly reduced.

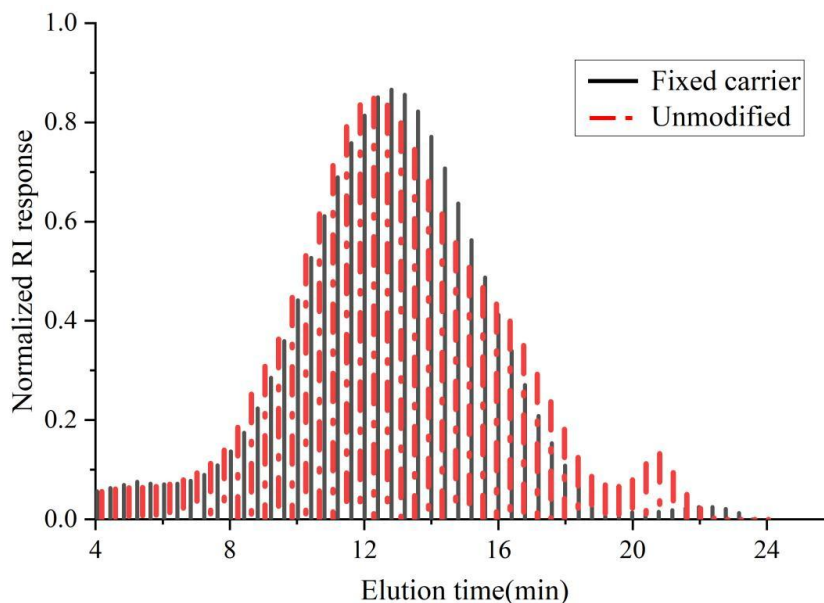


Figure 9: SEC spectrum after lipase degradation

5 Conclusion

In this paper, N-succinimidyl chitosan microspheres were produced by the reaction of succinic anhydride with chitosan, which was used as a carrier for the immobilization of lipase, and the resulting immobilized enzyme was used for the catalysis of long-chain fatty acid ester pollutants in water.

(1) The acylation reaction occurred at the $-NH_2$ position in the chitosan molecule, and the appearance of the $-NH-CO$ structure in the product was clearly seen in the Fourier infrared spectrum. The resonance peaks and shifts on the NMR spectra likewise verified the occurrence of the N-acylation reaction.

(2) One-way experiments on pH and cross-linking reaction temperature showed that the pH of the phosphate solution was highest at 7.5 for the transesterification ratio activity of the immobilized lipase. And at the same pH value, the reaction temperature with the highest transesterification specific activity was 48°C .

(3) The degradation catalytic efficiency of immobilized lipase was significantly higher than that of free lipase at the same hydrolysis time. And, when the reaction duration reached 3.5 h, the degradation efficiency was instead still higher than that in the initial 40 min.

About the Author

Yan Zhu (Oct. 1985-), male, Han ethnicity, native of Yangzhou, Jiangsu Province. He holds a doctoral degree and works as a lecturer at the School of Resources and Environmental Engineering, Yangzhou Polytechnic University. His main research directions include carrier synthesis, enzyme catalysis, and aquatic environmental pollution control.

References

- [1] Bielen, A., Šimatović, A., Kosić-Vukšić, J., Senta, I., Ahel, M., Babić, S., ... & Udiković-Kolić, N. (2017). Negative environmental impacts of antibiotic-contaminated effluents from pharmaceutical industries. *Water research*, 126, 79-87.
- [2] Issakhov, A., Alimbek, A., & Zhandaulet, Y. (2021). The assessment of water pollution by chemical reaction products from the activities of industrial facilities: Numerical study. *Journal of Cleaner Production*, 282, 125239.
- [3] Salim Dantas, M., Rodrigues Barroso, G., & Corrêa Oliveira, S. (2021). Performance of sewage treatment plants and impact of effluent discharge on receiving water quality within an urbanized area. *Environmental Monitoring and Assessment*, 193(5), 289.
- [4] Zahoor, I., & Mushtaq, A. (2023). Water pollution from agricultural activities: A critical global review. *Int. J. Chem. Biochem. Sci*, 23(1), 164-176.
- [5] Hassan, M., Hassan, R., Mahmud, M. A., Pia, H. I., Hassan, M. A., & Uddin, M. J. (2017). Sewage waste water characteristics and its management in urban areas-A case study at pagla sewage treatment plant, dhaka. *Urban and Regional Planning*, 2(3), 13.
- [6] Yu, Q., Liu, R., Chen, J., & Chen, L. (2019). Electrical conductivity in rural domestic sewage: An indication for comprehensive concentrations of influent pollutants and the effectiveness of treatment facilities. *International Biodeterioration & Biodegradation*, 143, 104719.
- [7] Hanafi, M. F., & Sapawe, N. (2020). A review on the current techniques and technologies of organic pollutants removal from water/wastewater. *Materials Today: Proceedings*, 31, A158-A165.
- [8] Zhang, K., Cheng, F., Zhang, K., Hu, J., Xu, C., Lin, Y., ... & Zhu, P. (2019). Synthesis of long-chain fatty acid starch esters in aqueous medium and its characterization. *European Polymer Journal*, 119, 136-147.
- [9] Luo, Y., Wang, Y., Guo, F., Kainz, M. J., You, J., Li, F., ... & Zhang, Y. (2024). Sources and fate of omega-3 polyunsaturated fatty acids in a highly eutrophic lake. *Science of the Total Environment*, 932, 172879.
- [10] Gonçalves, A. M., & Marques, J. C. (2017). Fatty Acids' Profiles of Aquatic Organisms: Revealing. *Fatty acids*, 89.
- [11] Sun, M., Shi, Z., Zhang, C., Zhang, Y., Zhang, S., & Luo, G. (2022). Novel long-chain fatty acid (LCFA)-degrading bacteria and pathways in anaerobic digestion promoted by hydrochar as revealed by genome-centric metatranscriptomics analysis. *Applied and Environmental Microbiology*, 88(16), e01042-22.
- [12] Bilal, M., Bagheri, A. R., Vilar, D. S., Aramesh, N., Eguiluz, K. I. B., Ferreira, L. F. R., ... & Iqbal, H. M. (2022). Oxidoreductases as a versatile biocatalytic tool to tackle pollutants for clean environment—a review. *Journal of Chemical Technology & Biotechnology*, 97(2), 420-435.

- [13] Bilal, M., Zhao, Y., Noreen, S., Shah, S. Z. H., Bharagava, R. N., & Iqbal, H. M. (2019). Modifying bio-catalytic properties of enzymes for efficient biocatalysis: A review from immobilization strategies viewpoint. *Biocatalysis and Biotransformation*, 37(3), 159-182.
- [14] Kate, A., Sahu, L. K., Pandey, J., Mishra, M., & Sharma, P. K. (2022). Green catalysis for chemical transformation: The need for the sustainable development. *Current Research in Green and Sustainable Chemistry*, 5, 100248.
- [15] Maghraby, Y. R., El-Shabasy, R. M., Ibrahim, A. H., & Azzazy, H. M. E. S. (2023). Enzyme immobilization technologies and industrial applications. *ACS omega*, 8(6), 5184-5196.
- [16] Liu, Y., & Dave, D. (2022). Recent progress on immobilization technology in enzymatic conversion of marine by-products to concentrated omega-3 fatty acids. *Green Chemistry*, 24(3), 1049-1066.
- [17] Alzahrani, A. A., Krayem, N., Alonazi, M., Al-Shehri, E., Horchani, H., & Bacha, A. B. (2025). Efficient Immobilization of Lipase for Sustainable Lipid Degradation and Wastewater Bioremediation. *ACS Omega*, 10(25), 26913.
- [18] Zong, W., Su, W., Xie, Q., Gu, Q., Deng, X., Ren, Y., & Li, H. (2022). Expression, characterization, and immobilization of a novel SGNH esterase Est882 and its potential for pyrethroid degradation. *Frontiers in Microbiology*, 13, 1069754.
- [19] Işık, C., Saraç, N., Teke, M., & Uğur, A. (2021). A new bioremediation method for removal of wastewater containing oils with high oleic acid composition: *Acinetobacter haemolyticus* lipase immobilized on eggshell membrane with improved stabilities. *New Journal of Chemistry*, 45(4), 1984-1992.
- [20] Cui, S., Zhou, Q. W., Wang, X. L., Yang, S. Q., Chen, K., Dai, Z. Y., ... & Zhou, T. (2017). Immobilization of lipase onto N-succinyl-chitosan beads and its application in the enrichment of polyunsaturated fatty acids in fish oil. *Journal of Food Biochemistry*, 41(5), e12395.
- [21] Tu, N., Shou, J., Dong, H., Huang, J., & Li, Y. (2017). Improved catalytic performance of lipase supported on clay/chitosan composite beads. *Catalysts*, 7(10), 302.
- [22] Melo, A. D., Silva, F. F., Dos Santos, J. C., Fernández-Lafuente, R., Lemos, T. L., & Dias Filho, F. A. (2017). Synthesis of benzyl acetate catalyzed by lipase immobilized in nontoxic chitosan-polyphosphate beads. *Molecules*, 22(12), 2165.
- [23] Weng, M., Xia, C., Xu, S., Liu, Q., Liu, Y., Liu, H., ... & Miao, Z. (2022). Lipase/chitosan nanoparticle-stabilized pickering emulsion for enzyme catalysis. *Colloid and Polymer Science*, 300(1), 41-50.
- [24] Pereira, A. D. S., Diniz, M. M., De Jong, G., Gama Filho, H. S., Dos Anjos, M. J., Finotelli, P. V., ... & Amaral, P. F. (2019). Chitosan-alginate beads as encapsulating agents for *Yarrowia lipolytica* lipase: Morphological, physico-chemical and kinetic characteristics. *International journal of biological macromolecules*, 139, 621-630.
- [25] Costa-Silva, T. A., Carvalho, A. K. F. D., Souza, C. R. F. D., De Castro, H. F., Bachmann,

- L., Said, S., & Oliveira, W. P. D. (2021). Enhancement lipase activity via immobilization onto chitosan beads used as seed particles during fluidized bed drying: Application in butyl butyrate production. *Applied Catalysis A: General*, 622, 118217.
- [26] Akil, E., Pereira, A. D. S., El-Bacha, T., Amaral, P. F., & Torres, A. G. (2020). Efficient production of bioactive structured lipids by fast acidolysis catalyzed by *Yarrowia lipolytica* lipase, free and immobilized in chitosan-alginate beads, in solvent-free medium. *International Journal of Biological Macromolecules*, 163, 910-918.
- [27] Liu, Y. W., Zhou, Y., Huang, G. Q., Guo, L. P., Li, X. D., & Xiao, J. X. (2022). Fabrication of lipase-loaded particles by coacervation with chitosan. *Food Chemistry*, 385, 132689.
- [28] Wei, H., Wang, Q., Zhang, R., Liu, M., & Zhang, W. (2023). Efficient biodiesel production from waste cooking oil by fast co-immobilization of lipases from *Aspergillus oryzae* and *Rhizomucor miehei* in magnetic chitosan microcapsules. *Process Biochemistry*, 125, 171-180.
- [29] Ribeiro, E. S., Machado, B. R., de Farias, B. S., dos Santos, L. O., Duarte, S. H., Cadaval Junior, T. R. S. A., ... & Diaz, P. S. (2024). Development of Microstructured Chitosan Nanocapsules with Immobilized Lipase. *Journal of Polymers and the Environment*, 32(8), 3627-3639.
- [30] Charuwat, P., Boardman, G., Bott, C., & Novak, J. T. (2018). Thermal Degradation of Long Chain Fatty Acids: Charuwat et al. *Water Environment Research*, 90(3), 278-287.